Phasing of millennial-scale climate variability in the Pacific and Atlantic Oceans

Maureen H. Walczak[1,2]*, Alan C. Mix[1], Ellen A. Cowan[3], Stewart Fallon[2], L. Keith Fifield[2], Jay R. Alder[1,4]†, Jianghui Du[1,5]†, Brian Haley[1]†, Tim Hobern[2]†, June Padman[1]†, Summer K. Praetorius[6]†, Andreas Schmittner[1]†, Joseph S. Stoner[1]†, Sarah D. Zellers[7]†

[1]College of Earth, Ocean, and Atmospheric Sciences, Oregon State University, Corvallis, OR, USA. [2]Australian National University, Canberra ACT. [3]Department of Geological and Environmental Sciences, Appalachian State University, Boone, NC, USA. [4]United States Geological Survey, Corvallis, OR, USA. [5]Department of Earth Sciences, Institute of Geochemistry and Petrology, ETH Zurich, Zurich, Switzerland. [6]United States Geological Survey, Menlo Park, CA, USA. [7]University of Central Missouri, Warrensburg, MO, USA.

*Corresponding author. E-mail: mo.walczak@oregonstate.edu

†These authors contributed equally to this work.

New radiocarbon and sedimentological results from the Gulf of Alaska document recurrent millennial-scale episodes of reorganized Pacific Ocean ventilation synchronous with rapid Cordilleran Ice Sheet discharge, indicating close coupling of ice-ocean dynamics spanning the past 42,000 years. Ventilation of the intermediate-depth North Pacific tracks strength of the Asian Monsoon, supporting a role for moisture and heat transport from low-latitudes in North Pacific paleoclimate. Changes in ^{14}C age of intermediate waters are in phase with peaks in Cordilleran ice-rafted debris delivery, and both consistently precede ice discharge events from the Laurentide Ice Sheet, known as Heinrich Events. This timing precludes an Atlantic trigger for Cordilleran Ice Sheet retreat, and instead implicates the Pacific as an early part of a cascade of dynamic climate events with global impact.

During the last glacial period the Laurentide Ice Sheet of North America experienced recurrent, unstable millennial-scale retreat events, characterized by episodic iceberg discharge inferred from the presence of apparently ice-rafted detrital sedimentary layers far into the Atlantic Ocean (*1*). These so-called Heinrich Events are among the most abrupt climate perturbations of Earth's recent past (*2*). Various triggering mechanisms have been theorized, including reduction of the Atlantic Meridional Overturning Circulation (AMOC (*3*)) warming of subsurface waters (*4–6*), internal dynamics of the large Laurentide Ice Sheet (*7*), and/or sea-level rise triggered by episodic failure of another (presumably European) ice sheet (*8*). Regardless of origin, changes in oceanic and atmospheric circulation associated with the Heinrich Events correspond to global perturbations including weak intervals of the Asian Monsoon (*9*), and antiphased warming in Antarctica (*10*).

Marine sedimentary records spanning the Northeast Pacific document periods of high ice discharge analogous to the Heinrich Events off the west coast of North America, but with uncertain timing and cause (*11–14*). Here, based on a detailed radiocarbon chronology in the Gulf of Alaska, we assess the timing of the Pacific ice discharge events from the Cordilleran Ice Sheet and changes in apparent subsurface ocean radiocarbon ages, and establish phasing relationships between North Pacific and North Atlantic events. We find that Pacific discharge events and intermediate water ventilation changes

precede events in the North Atlantic, and are early parts of a dynamic cascade of global climate changes including Antarctic warming and atmospheric CO_2 rise. We thus reject hypotheses that these North Pacific millennial-scale climate events originate as passive teleconnected responses to the Laurentide/North Atlantic or Antarctic.

During the last glacial period the Alaskan margin hosted ice streams draining the northwestern limb of the Cordilleran Ice Sheet, evidenced by a series of sedimented troughs crossing the continental shelf (*15*). Although smaller than the Laurentide Ice Sheet, the Cordilleran Ice Sheet at its Last Glacial Maximum (LGM) extent was slightly larger than the modern-day Greenland Ice Sheet (*16*). IODP Site U1419 (59° 31.9'N, 144° 8.0'W, 690 m water depth; Fig. 1) was drilled on the Gulf of Alaska slope in ~690 m water depth on the continental slope ~75 km seaward of the Bering Glacier, a modern remnant of a major ice stream that may have routed ~15% of drainage from the Cordilleran Ice Sheet (fig. S1). Four drill holes yielded a continuous stratigraphic splice extending back >90 m adjusted composite depth below seafloor, CCSF-B; (*17*).

A Bayesian age model based on 250 ^{14}C measurements of planktic and benthic foraminifera, and limited correlation points beyond the range of ^{14}C (table S1 and fig. S2) indicates the base of the stratigraphic splice was deposited ~55,000 years before present (BP) (tables S3 and S4 and Fig. 2). The chronology discussed here is based on calibration of

radiocarbon dates using the Marine13 curve (*18*), however our conclusions are insensitive to calibration on the Marine20 curve (*19*) and that alternate age model is presented and discussed in Supplementary Materials. Corrected ages and sediment accumulation rates, and their uncertainties, are resolved in 500-year intervals to ~60,000 BP (tables S4 and S5). Accumulation rates range from as low as ~10 cm/kyr in mid Holocene time (average 50 ± 30 cm/kyr, 0-11,700 BP) to peaks of ~800 cm/kyr during ice discharge events of the latest Pleistocene (average 200 ± 160 cm/kyr, 12,000-50,000 BP; fig. S3).

Each interval of anomalously high sediment accumulation rate off SE Alaska contains a high concentration of coarse (sand-size or greater) grains not associated with turbidites, interpreted as ice-rafted detritus (IRD) (See Materials and Methods). Mean IRD mass accumulation rates (MAR) range from zero (indicating glaciers retreated from the ocean either onto land or behind fjord sills sufficiently shallow to inhibit iceberg fluxes) to as high as 40 g cm^{-2} kyr^{-1}. We name these episodes of high IRD MAR '*Siku Events*' (the Inupiat/Inuit word for ice, abbreviated here as "S Events"), which we define operationally as IRD MAR >*12* g cm^{-2} kyr^{-1} averaged over a time span of *500* years or longer. This definition yields events S1 (peak at 17.0-18.0 kyr BP), S2 (25.0-27.0 kyr BP), S3 (29.5-30.5 kyr BP), S4 (39.5-42.0 kyr BP), and perhaps S5 (~54-56 kyr BP, although the age model and IRD MAR is imprecise in this interval) (Fig. 3 and fig. S9). The Siku Events represent a massive influx of icebergs from regional retreat of marine-terminating outlet glaciers from the Cordilleran Ice Sheet. This association is analogous to that of North Atlantic Heinrich Events (*20*), and is consistent with evidence for anomalously high sediment fluxes associated with recent tidewater glacier retreat in Alaska (*21*).

The lithology of IRD grains at Site U1419 varies widely, reflecting both proximal sources in the Chugach and St. Elias Ranges drained by the Bering Glacier as well as more distal sources including the Alexander terrane of SE Alaska and western British Columbia (*17*). This diversity of provenance suggests that sediments from the northern Gulf of Alaska integrate ice rafted detritus from the western Cordilleran ice streams, carried northward and westward by the Alaska Current and Alaska Coastal Current. Meltwater influx likely accelerates these current systems during episodes of rapid ice retreat (*22*). The youngest Siku event (S1) captured in the U1419 marine IRD record coincides with terrestrial cosmogenic-exposure dates for retreat of the western Cordilleran, roughly synchronous on the marine margin from Alaska to southern British Columbia (*23, 24*).

The modern water mass at the depth of Site U1419 is at the approximate boundary of North Pacific Intermediate Water (NPIW; an intermediate watermass partially ventilated to the atmosphere in the Sea of Okhotsk (*25*)) and Pacific Deep Water (PDW; a primary watermass sourced around Antarctica as Circumpolar Deep Water with relatively high preformed ^{14}C age, transited northward from the southern ocean near the sea floor as Antarctic Bottom Water and returned southward at mid depths, mixing with overlying waters but without interacting with the atmosphere (*26*)). A ^{14}C-depleted watermass expanded through much of the deep Pacific during the most recent glacial termination (*27*), with high apparent ages at intermediate depths approximately coeval with two events of increased benthic reservoir age observed in the Gulf of Alaska (*28*). These events, associated with deglacial increases in atmospheric CO_2, have been inferred to reflect the upward mixing and redistribution of a ^{14}C-depleted deep watermass (*29, 30*). Evidence from authigenic εNd provides further support for the interpretation of an increased contribution of abyssal Pacific waters to intermediate-depth North Pacific waters at these times (*31, 32*).

We measured 82 benthic-planktic (B-P) radiocarbon pairs spanning the past ~50,000 years BP at Site U1419, overlapping with and extending 28 paired measurements from <18,000 calibrated ^{14}C years before present (cal BP) in co-located core EW0408-85JC (59° 33.32'N, 144° 9.21'W, 682 m (*28, 33*)) (fig. S2). At this site, an increase in the radiocarbon age of bottom waters relative to the surface (e.g., high B-P values) may indicate: a) decreased circulation rate increasing the true age of subsurface waters, b) decreased gas exchange of source waters imparting an apparently high preformed age on the watermass, c) shoaling or increased mixing of underlying ^{14}C-deficient deep waters with overlying intermediate waters, and/or d) decreased mixing of intermediate waters with the sea surface (for example via enhanced shallow stratification (*34*)). The largest B-P age excursions observed here cannot be driven solely by decreases in surface age (for example by less mixing with underlying older waters or greater effective local gas exchange) as this would require implausible surface water ages younger than the coeval atmosphere (*28*). Thus, substantial increases of B-P age differences must reflect increases in subsurface reservoir ages.

We limit the evaluation of the B-P at Site U1419 to ages <42,000 cal BP (76.5 m CCSF-B), where analytical precision is sufficient for meaningful interpretation (see Materials and Methods). The B-P age differences over that interval average 790 ± 340 (1σ) years, similar to (but with broader range than) the site's average Holocene (<11,700) value of 750 ± 120 (1σ) years (*28*), and estimated modern pre-bomb ^{14}C age differences between surface and intermediate waters of 675 ± 90 (1σ) years (*35*). Over the past 42,000 cal BP, four identifiable episodes occur in which B-P age differences exceed 1000 years (confirmed by 2 or more B-P pairs), centered at 12,800, 17,700, 25,600, and 40,600 cal BP (Fig. 3). The older three of these episodes of high B-P are synchronous with Siku Events 1, 2, and 4.

A smaller Siku Event (S3), potentially associated with H3 near 30,000 cal BP, has no accompanying B-P anomaly at Site U1419 (Fig. 3). However, in this interval the resolution of the ^{14}C data set is low, so an event may have been missed here. The youngest B-P excursion (~12,800 cal BP), previously identified in nearby core EW0408-85JC (28), does not correspond to a Siku Event as expressed in IRD, but it is associated with terrestrial ice retreat ((36–38), high meltwater fluxes from land and adjacent surface ocean cooling (33, 39). By this time the Cordilleran outlet glaciers had retreated into silled fjords (36) that served as sediment traps, leaving little expression of enhanced sediment or IRD fluxes in the open ocean (40).

The North Pacific may be sensitive to the Asian Monsoon, which provides a net freshwater source that contributes to upper ocean stratification, limiting subsurface ventilation (41). High B-P and Siku Events are initiated during strong monsoon intervals (higher net freshwater flux to the North Pacific), while low B-P events tend to occur in concert with weak monsoons (which are coincident with Atlantic Heinrich Events; Fig. 4). Northward heat transport associated with strong monsoons may contribute to net negative mass balance and retreat of the marine margin of the Cordilleran Ice Sheet (42). In turn, freshwater discharge from the Cordilleran Ice Sheet can further stratify the NE Pacific, allow intermediate water reservoir ages to rise as vertical mixing with the surface ocean is suppressed and mixing with the deep ocean is favored, while triggering dynamic responses in the North Atlantic sector (14, 39, 43, 44). Chinese Cave δ^{18}O (9) leads Siku Events by ~1000-3000 years (Fig. 4), reasonable for an ice sheet response to warming. This would seemingly support the hypothesis that low-latitude processes are an important driver of high-latitude climate (45).

Antarctic warming, as reconstructed from ice core δ^{18}O, follows within ~1000 years of Siku Events, with peak warmth ~2500 years after peak IRD MAR (Figs. 3 and 5). This phasing appears to preclude northward propagation of an Antarctic trigger for Siku Events (3), but could support a mechanism in which Cordilleran meltwater cools the North Pacific and in turn the North Atlantic, whereby reduction in Atlantic Meridional Overturning Circulation (AMOC) triggers Antarctic warming (43). Changes in Southern and Pacific Ocean circulation associated with Antarctic warming during the Heinrich Events are hypothesized to be related to the release of carbon from the interior ocean, driving some portion of the following increase in atmospheric CO_2 (32, 46) (Fig. 5).

Atlantic Heinrich Events lag Pacific Siku Events by 1370 ± 550 years for peak IRD. This phasing precludes teleconnection mechanisms in which Atlantic processes trigger the earlier expression of Pacific millennial-scale climate instability (Fig. 5 and fig. S10). The correspondence of high North Pacific B-P age differences with Siku events similarly precludes their origin as a down-stream reduction of Pacific intermediate-water ventilation in response to AMOC suppression during Heinrich Events.

Although high B-P age differences in the North Pacific precede Heinrich Events, the lowest B-P age differences at Site U1419 co-occur with H0, H1, H2, and H4, and may plausibly reflect the regional response to Heinrich Events (Fig. 3). Similar timing for low B-P is found in the NW Pacific and Bering Sea (47–51), and may support a hypothesized inter-ocean "see-saw" effect in shallow subsurface ventilation (52–54). Earth system model results suggest freshwater input in the North Atlantic during Heinrich Events could drive invigorated NPIW production and/or enhanced stratification between NPIW and PDW, both of which would contribute to younger intermediate water age (55, 56).

We have documented correspondence of increased NE Pacific intermediate water ^{14}C ages and ice rafted debris delivery during the past 42,000 years. A finely resolved chronology implicates Cordilleran ice retreat (Siku Events) as early in a chain of prominent climate events, following strong Asian Monsoons but leading the Heinrich Events of the North Atlantic, Antarctic warming, and global CO_2 rise (Fig. 5). These observations indicate that the Cordilleran Ice Sheet and North Pacific Ocean play an active role in millennial-scale climate oscillations, and precludes direct forcing of Cordilleran ice retreat from Heinrich Events. Mechanisms linking Pacific and Atlantic ice retreat events may include atmospheric heat transports and adjustments in the Arctic (44), net freshwater transports from the Pacific to the Atlantic when Bering Strait is open (39), and/or rapid sea-level rises accompanying ice melt. Precursor retreat of the smaller European ice sheets, posited as a trigger for Laurentide ice purges (8), has since been discounted (1). However, the early and rapid Cordilleran ice losses documented here are more likely to influence Atlantic ice sheet retreat. The relative response times of these various interacting systems range from sub-decadal (monsoons and atmospheric adjustments), centuries (smaller Cordilleran ice and watermass ventilation), to millennia (larger Laurentide ice and inter-basin deep circulation), offering a possibility that linkages across a range of timescales could drive auto-oscillating behavior when ice is present as a triggering mechanism (57).

REFERENCES AND NOTES

1. S. R. Hemming, Heinrich events: Massive late Pleistocene detritus layers of the North Atlantic and their global climate imprint. *Rev. Geophys.* **42**, RG1005 (2004). doi:10.1029/2003RG000128

2. W. S. Broecker, Massive iceberg discharges as triggers for global climate change. *Nature* **372**, 421–424 (1994). doi:10.1038/372421a0

3. P. U. Clark, S. W. Hostetler, K. J. Meissner, N. G. Pisias, A. Schmittner, in *Ocean Circulation: Mechanisms and Impacts - Past and Future Changes of Meridional Overturning*, A. Schmittner, J. C. H. Chiang, S. R. Hemming, Eds., Geophysical Monograph 173 (American Geophysical Union, 2007), pp. 209–246.

4. G. Shaffer, S. M. Olsen, C. J. Bjerrum, Ocean subsurface warming as a mechanism for coupling Dansgaard-Oeschger climate cycles and ice-rafting events. *Geophys. Res. Lett.* **31**, L24202 (2004). doi:10.1029/2004GL020968

5. S. A. Marcott, P. U. Clark, L. Padman, G. P. Klinkhammer, S. R. Springer, Z. Liu, B. L. Otto-Bliesner, A. E. Carlson, A. Ungerer, J. Padman, F. He, J. Cheng, A. Schmittner, Ice-shelf collapse from subsurface warming as a trigger for Heinrich events. *Proc. Natl. Acad. Sci. U.S.A.* **108**, 13415–13419 (2011). doi:10.1073/pnas.1104772108 Medline

6. J. N. Bassis, S. V. Petersen, L. Mac Cathles, Heinrich events triggered by ocean forcing and modulated by isostatic adjustment. *Nature* **542**, 332–334 (2017). doi:10.1038/nature21069 Medline

7. D. R. MacAyeal, Binge/purge oscillations of the Laurentide Ice Sheet as a cause of the North Atlantic's Heinrich events. *Paleoceanography* **8**, 775–784 (1993). [doi:10.1029/93PA02200](doi:10.1029/93PA02200)

8. G. C. Bond, R. Lotti, Iceberg discharges into the north atlantic on millennial time scales during the last glaciation. *Science* **267**, 1005–1010 (1995). doi:10.1126/science.267.5200.1005 Medline

9. H. Cheng, R. L. Edwards, A. Sinha, C. Spötl, L. Yi, S. Chen, M. Kelly, G. Kathayat, X. Wang, X. Li, X. Kong, Y. Wang, Y. Ning, H. Zhang, The Asian monsoon over the past 640,000 years and ice age terminations. *Nature* **534**, 640–646 (2016). doi:10.1038/nature18591 Medline

10. T. Blunier, E. J. Brook, Timing of millennial-scale climate change in Antarctica and Greenland during the last glacial period. *Science* **291**, 109–112 (2001). doi:10.1126/science.291.5501.109 Medline

11. A. T. Hewitt, D. Mcdonald, B. D. Bornhold, Ice-rafted debris in the North Pacific and correlation to North Atlantic climatic events. *Geophys. Res. Lett.* **24**, 3261–3264 (1997). [doi:10.1029/97GL03264](doi:10.1029/97GL03264)

12. A. C. Mix, D. C. Lund, N. G. Pisias, P. Boden, L. Bornmalm, M. Lyle, J. Pike, in *Mechanisms of Global Climate Change at Millennial Time Scales*, Geophysical Monograph 112 (American Geophysical Union, 1999), pp. 127–148.

13. I. L. Hendy, T. Cosma, Vulnerability of the Cordilleran Ice Sheet to iceberg calving during late quaternary rapid climate change events. *Paleoceanography* **23**, PA2101 (2008). [doi:10.1029/2008PA001606](doi:10.1029/2008PA001606)

14. E. Maier, X. Zhang, A. Abelmann, R. Gersonde, S. Mulitza, M. Werner, M. Méheust, J. Ren, B. Chapligin, H. Meyer, R. Stein, R. Tiedemann, G. Lohmann, North Pacific freshwater events linked to changes in glacial ocean circulation. *Nature* **559**, 241–245 (2018). [doi:10.1038/s41586-018-0276-y](doi:10.1038/s41586-018-0276-y) Medline

15. J. M. Swartz, S. P. S. Gulick, J. A. Goff, Gulf of Alaska continental slope morphology: Evidence for recent trough mouth fan formation. *Geochem. Geophys. Geosyst.* **16**, 165–177 (2015). [doi:10.1002/2014GC005594](doi:10.1002/2014GC005594)

16. J. Seguinot, I. Rogozhina, A. P. Stroeven, M. Margold, J. Kleman, Numerical simulations of the Cordilleran ice sheet through the last glacial cycle. *Cryosphere* **10**, 639–664 (2016). [doi:10.5194/tc-10-639-2016](doi:10.5194/tc-10-639-2016)

17. J. M. Jaeger, S. P. S. Gulick, L. J. LeVay, H. Asahi, H. Bahlburg, C. L. Belanger, G. B. B. Berbel, L. B. Childress, E. A. Cowan, L. Drab, M. Forwick, A. Fukumura, S. Ge, S. M. Gupta, A. Kioka, S. Konno, C. E. März, K. M. Matsuzaki, E. L. McClymont, A. C. Mix, C. M. Moy, J. Müller, A. Nakamura, T. Ojima, K. D. Ridgway, F. Rodrigues Ribeiro, O. E. Romero, A. L. Slagle, J. S. Stoner, G. St-Onge, I. Suto, M. H. Walczak, L. L. Worthington, Expedition 341 summary, in *Proc. IODP*, 341, J. M. Jaeger, S. P. S. Gulick, L. J. LeVay, and the Expedition 341 Scientists (Integrated Ocean Drilling Program, College Station, TX, 2014). doi:10.2204/iodp.pr.341.2014.

18. P. J. Reimer, E. Bard, A. Bayliss, J. W. Beck, P. G. Blackwell, C. B. Ramsey, C. E. Buck, H. Cheng, R. L. Edwards, M. Friedrich, P. M. Grootes, T. P. Guilderson, H. Haflidason, I. Hajdas, C. Hatté, T. J. Heaton, D. L. Hoffmann, A. G. Hogg, K. A. Hughen, K. F. Kaiser, B. Kromer, S. W. Manning, M. Niu, R. W. Reimer, D. A. Richards, E. M. Scott, J. R. Southon, R. A. Staff, C. S. M. Turney, J. van der Plicht, IntCal13 and Marine13 Radiocarbon Age Calibration Curves 0–50,000 Years cal BP. *Radiocarbon* **55**, 1869–1887 (2013). [doi:10.2458/azu_js_rc.55.16947](doi:10.2458/azu_js_rc.55.16947)

19. T. J. Heaton, P. Köhler, M. Butzin, E. Bard, R. W. Reimer, W. E. N. Austin, C. Bronk Ramsey, P. M. Grootes, K. A. Hughen, B. Kromer, P. J. Reimer, J. Adkins, A. Burke, M. S. Cook, J. Olsen, L. C. Skinner, Marine20—the marine radiocarbon age calibration curve (0–55,000 CAL BP). *Radiocarbon* **62**, 779–820 (2020). [doi:10.1017/RDC.2020.68](doi:10.1017/RDC.2020.68)

20. S. J. Marshall, M. R. Koutnik, Ice sheet action versus reaction: Distinguishing between Heinrich events and Dansgaard-Oeschger cycles in the North Atlantic. *Paleoceanography* **21**, PA2021 (2006). [doi:10.1029/2005PA001247](doi:10.1029/2005PA001247)

21. M. N. Koppes, B. Hallet, Influence of rapid glacial retreat on the rate of erosion by tidewater glaciers. *Geology* **30**, 47–50 (2002). doi:10.1130/0091-7613(2002)030<0047:IORGRO>2.0.CO;2

22. T. C. Royer, B. Finney, An oceanographic perspective on early human migrations to the Americas. *Oceanography (Wash. D.C.)* **33**, (2020). doi:10.5670/oceanog.2020.102

23. C. M. Darvill, B. Menounos, B. M. Goehring, O. B. Lian, M. W. Caffee, Retreat of the Western Cordilleran Ice Sheet Margin During the Last Deglaciation. *Geophys. Res. Lett.* **45**, 9710–9720 (2018). [doi:10.1029/2018GL079419](doi:10.1029/2018GL079419)

24. A. J. Lesnek, J. P. Briner, C. Lindqvist, J. F. Baichtal, T. H. Heaton, Deglaciation of the Pacific coastal corridor directly preceded the human colonization of the Americas. *Sci. Adv.* **4**, eaar5040 (2018). doi:10.1126/sciadv.aar5040 Medline

25. L. D. Talley, Distribution and Formation of North Pacific Intermediate Water. *J. Phys. Oceanogr.* **23**, 517–537 (1993). doi:10.1175/1520-0485(1993)023<0517:DAFONP>2.0.CO;2

26. L. D. Talley, Closure of the Global Overturning Circulation Through the Indian, Pacific, and Southern Oceans: Schematics and Transports. *Oceanography (Wash. D.C.)* **26**, 80–97 (2013). doi:10.5670/oceanog.2013.07

27. T. M. Marchitto, S. J. Lehman, J. D. Ortiz, J. Flückiger, A. van Geen, Marine radiocarbon evidence for the mechanism of deglacial atmospheric CO_2 rise. *Science* **316**, 1456–1459 (2007). doi:10.1126/science.1138679 Medline

28. M. Davies-Walczak, A. C. Mix, J. S. Stoner, J. R. Southon, M. Cheseby, C. Xuan, Late Glacial to Holocene radiocarbon constraints on North Pacific Intermediate Water ventilation and deglacial atmospheric CO_2 sources. *Earth Planet. Sci. Lett.* **397**, 57–66 (2014). doi:10.1016/j.epsl.2014.04.004

29. E. L. Sikes, C. R. Samson, T. P. Guilderson, W. R. Howard, Old radiocarbon ages in the southwest Pacific Ocean during the last glacial period and deglaciation. *Nature* **405**, 555–559 (2000). [doi:10.1038/35014581](doi:10.1038/35014581) Medline

30. L. Skinner, I. N. McCave, L. Carter, S. Fallon, A. E. Scrivner, F. Primeau, Reduced ventilation and enhanced magnitude of the deep Pacific carbon pool during the last glacial period. *Earth Planet. Sci. Lett.* **411**, 45–52 (2015). doi:10.1016/j.epsl.2014.11.024

31. C. Basak, E. E. Martin, K. Horikawa, T. M. Marchitto, Southern Ocean source of ^{14}C-depleted carbon in the North Pacific Ocean during the last deglaciation. *Nat. Geosci.* **3**, 770–773 (2010). doi:10.1038/ngeo987

32. J. Du, B. A. Haley, A. C. Mix, M. H. Walczak, S. K. Praetorius, Flushing of the deep Pacific Ocean and the deglacial rise of atmospheric CO_2 concentrations. *Nat. Geosci.* **11**, 749–755 (2018). [doi:10.1038/s41561-018-0205-6](doi:10.1038/s41561-018-0205-6)

33. M. H. Davies, A. C. Mix, J. S. Stoner, J. A. Addison, J. Jaeger, B. Finney, J. Wiest, The deglacial transition on the southeastern Alaska Margin: Meltwater input, sea level rise, marine productivity, and sedimentary anoxia. *Paleoceanography* **26**, PA2223 (2011). [doi:10.1029/2010PA002051](doi:10.1029/2010PA002051)

34. S. Khatiwala, F. Primeau, M. Holzer, Ventilation of the deep ocean constrained with tracer observations and implications for radiocarbon estimates of ideal mean age. *Earth Planet. Sci. Lett.* **325-326**, 116–125 (2012). doi:10.1016/j.epsl.2012.01.038

35. R. M. Key, A. Kozyr, C. L. Sabine, K. Lee, R. Wanninkhof, J. L. Bullister, R. A. Feely, F. J. Millero, C. Mordy, T. H. Peng, A global ocean carbon climatology: Results from Global Data Analysis Project (GLODAP). *Global Biogeochem. Cycles* **18**, GB4031 (2004). [doi:10.1029/2004GB002247](doi:10.1029/2004GB002247)

36. B. Menounos, B. M. Goehring, G. Osborn, M. Margold, B. Ward, J. Bond, G. K. C. Clarke, J. J. Clague, T. Lakeman, J. Koch, M. W. Caffee, J. Gosse, A. P. Stroeven, J. Seguinot, J. Heyman, Cordilleran Ice Sheet mass loss preceded climate reversals near the Pleistocene Termination. *Science* **358**, 781–784 (2017). doi:10.1126/science.aan3001 Medline

37. J. P. Briner, D. S. Kaufman, Late Pleistocene mountain glaciation in Alaska: Key chronologies. *J. Quat. Sci.* **23**, 659–670 (2008). [doi:10.1002/jqs.1196](doi:10.1002/jqs.1196)

38. D. S. Kaufman, R. Scott Anderson, F. S. Hu, E. Berg, A. Werner, Evidence for a variable and wet Younger Dryas in southern Alaska. *Quat. Sci. Rev.* **29**, 1445–1452 (2010). doi:10.1016/j.quascirev.2010.02.025

39. S. K. Praetorius, A. Condron, A. C. Mix, M. H. Walczak, J. L. McKay, J. Du, The role of Northeast Pacific meltwater events in deglacial climate change. *Sci. Adv.* **6**, eaay2915 (2020). doi:10.1126/sciadv.aay2915 Medline

40. E. A. Cowan, K. C. Seramur, R. D. Powell, B. A. Willems, S. P. S. Gulick, J. M. Jaeger, Fjords as temporary sediment traps: History of glacial erosion and deposition in Muir Inlet, Glacier Bay National Park, southeastern Alaska. *Bull. Geol. Soc. Am.* **122**, 1067–1080 (2010). [doi:10.1130/B26595.1](doi:10.1130/B26595.1)

41. J. Emile-Geay, Warren revisited: Atmospheric freshwater fluxes and "Why is no

deep water formed in the North Pacific." *J. Geophys. Res.* **108**, 3178 (2003). doi:10.1029/2001JC001058

42. S. Hostetler, N. Pisias, A. Mix, Sensitivity of Last Glacial Maximum climate to uncertainties in tropical and subtropical ocean temperatures. *Quat. Sci. Rev.* **25**, 1168–1185 (2006). doi:10.1016/j.quascirev.2005.12.010

43. D. M. Roche, A. P. Wiersma, H. Renssen, A systematic study of the impact of freshwater pulses with respect to different geographical locations. *Clim. Dyn.* **34**, 997–1013 (2010). doi:10.1007/s00382-009-0578-8

44. S. Praetorius, M. Rugenstein, G. Persad, K. Caldeira, Global and Arctic climate sensitivity enhanced by changes in North Pacific heat flux. *Nat. Commun.* **9**, 3124 (2018). doi:10.1038/s41467-018-05337-8 Medline

45. J. W. Beck, W. Zhou, C. Li, Z. Wu, L. White, F. Xian, X. Kong, Z. An, A 550,000-year record of East Asian monsoon rainfall from [10]Be in loess. *Science* **360**, 877–881 (2018). doi:10.1126/science.aam5825 Medline

46. M. Sarnthein, B. Schneider, P. M. Grootes, Peak glacial ^{14}C ventilation ages suggest major draw-down of carbon into the abyssal ocean. *Clim. Past* **9**, 2595–2614 (2013). doi:10.5194/cp-9-2595-2013

47. N. Ahagon, Mid-depth circulation in the northwest Pacific during the last deglaciation: Evidence from foraminiferal radiocarbon ages. *Geophys. Res. Lett.* **30**, 2097 (2003). doi:10.1029/2003GL018287

48. Y. Okazaki, A. Timmermann, L. Menviel, N. Harada, A. Abe-Ouchi, M. O. Chikamoto, A. Mouchet, H. Asahi, Deepwater formation in the North Pacific during the Last Glacial Termination. *Science* **329**, 200–204 (2010). doi:10.1126/science.1190612 Medline

49. L. Max, L. Lembke-Jene, J. R. Riethdorf, R. Tiedemann, D. Nürnberg, H. Kühn, A. MacKensen, Pulses of enhanced north Pacific intermediate water ventilation from the Okhotsk Sea and Bering Sea during the last deglaciation. *Clim. Past* **10**, 591–605 (2014).

50. J. W. B. Rae, M. Sarnthein, G. L. Foster, A. Ridgewell, P. M. Grootes, T. Elliott, Deep water formation in the North Pacific and deglacial CO_2 rise. *Paleoceanography* **29**, 1–23 (2014).

51. W. R. Gray, J. W. B. Rae, R. C. J. Wills, A. E. Shevenell, B. Taylor, A. Burke, G. L. Foster, C. H. Lear, Deglacial upwelling, productivity and CO_2 outgassing in the North Pacific Ocean. *Nat. Geosci.* **11**, 1 (2018).

52. D. C. Lund, Deep Pacific ventilation ages during the last deglaciation: Evaluating the influence of diffusive mixing and source region reservoir age. *Earth Planet. Sci. Lett.* **381**, 52–62 (2013).

53. A. T. Kotilainen, N. J. Shackleton, Rapid climate variability in the North Pacific Ocean during the past 95,000 years. *Nature* **377**, 323–326 (1995). doi:10.1038/377323a0

54. O. A. Saenko, A. Schmittner, A. J. Weaver, The Atlantic – Pacific Seesaw. *J. Clim.* **17**, 2033–2038 (2004). doi:10.1175/1520-0442(2004)017<2033:TAS>2.0.CO:2

55. M. O. Chikamoto, L. Menviel, A. Abe-Ouchi, R. Ohgaito, A. Timmermann, Y. Okazaki, N. Harada, A. Oka, A. Mouchet, Variability in North Pacific intermediate and deep water ventilation during Heinrich events in two coupled climate models. *Deep. Res. Part II Top. Stud. Oceanogr.* **61–64**, 114–126 (2012).

56. X. Gong, L. Lembke-Jene, G. Lohmann, G. Knorr, R. Tiedemann, J. J. Zou, X. F. Shi, Enhanced North Pacific deep-ocean stratification by stronger intermediate water formation during Heinrich Stadial 1. *Nat. Commun.* **10**, 656 (2019). doi:10.1038/s41467-019-08606-2 Medline

57. M. Crucifix, Oscillators and relaxation phenomena in Pleistocene climate theory. *Philos. Trans. A Math. Phys. Eng. Sci.* **370**, 1140–1165 (2012). doi:10.1098/rsta.2011.0315 Medline

58. C. Amante, B. W. Eakins, ETOPO1 Global Relief Model converted to PanMap layer format. NOAA-National Geophysical Data Center, PANGAEA (2009). . https://doi.org/10.1594/PANGAEA.769615.

59. W. R. Peltier, D. F. Argus, R. Drummond, Space geodesy constrains ice age terminal deglaciation: The global ICE-6G-C (VM5a) model. *J. Geophys. Res. Solid Earth* **120**, 450–487 (2015). doi:10.1002/2014JB011176

60. R. McNeely, A. S. Dyke, J. R. Southon, Canadian marine reservoir ages: Preliminary data assessment. *Geol. Surv. Canada Open File* **5049** (2006). doi:10.13140/2.1.1461.6649

61. K. K. Andersen, N. Azuma, J. M. Barnola, M. Bigler, P. Biscaye, N. Caillon, J. Chappellaz, H. B. Clausen, D. Dahl-Jensen, H. Fischer, J. Flückiger, D. Fritzsche, Y. Fujii, K. Goto-Azuma, K. Grønvold, N. S. Gundestrup, M. Hansson, C. Huber, C. S.

Hvidberg, S. J. Johnsen, U. Jonsell, J. Jouzel, S. Kipfstuhl, A. Landais, M. Leuenberger, R. Lorrain, V. Masson-Delmotte, H. Miller, H. Motoyama, H. Narita, T. Popp, S. O. Rasmussen, D. Raynaud, R. Rothlisberger, U. Ruth, D. Samyn, J. Schwander, H. Shoji, M. L. Siggard-Andersen, J. P. Steffensen, T. Stocker, A. E. Sveinbjörnsdóttir, A. Svensson, M. Takata, J. L. Tison, T. Thorsteinsson, O. Watanabe, F. Wilhelms, J. W. White; North Greenland Ice Core Project members, High-resolution record of Northern Hemisphere climate extending into the last interglacial period. *Nature* **431**, 147–151 (2004). doi:10.1038/nature02805 Medline

62. L. Augustin, C. Barbante, P. R. Barnes, J. M. Barnola, M. Bigler, E. Castellano, O. Cattani, J. Chappellaz, D. Dahl-Jensen, B. Delmonte, G. Dreyfus, G. Durand, S. Falourd, H. Fischer, J. Flückiger, M. E. Hansson, P. Huybrechts, G. Jugie, S. J. Johnsen, J. Jouzel, P. Kaufmann, J. Kipfstuhl, F. Lambert, V. Y. Lipenkov, G. C. Littot, A. Longinelli, R. Lorrain, V. Maggi, V. Masson-Delmotte, H. Miller, R. Mulvaney, J. Oerlemans, H. Oerter, G. Orombelli, F. Parrenin, D. A. Peel, J. R. Petit, D. Raynaud, C. Ritz, U. Ruth, J. Schwander, U. Siegenthaler, R. Souchez, B. Stauffer, J. P. Steffensen, B. Stenni, T. F. Stocker, I. E. Tabacco, R. Udisti, R. S. Van De Wal, M. Van Den Broeke, J. Weiss, F. Wilhelms, J. G. Winther, E. W. Wolff, M. Zucchelli; EPICA community members, Eight glacial cycles from an Antarctic ice core. *Nature* **429**, 623–628 (2004). doi:10.1038/nature02599 Medline

63. D. Veres, L. Bazin, A. Landais, H. Toyé Mahamadou Kele, B. Lemieux-Dudon, F. Parrenin, P. Martinerie, E. Blayo, T. Blunier, E. Capron, J. Chappellaz, S. O. Rasmussen, M. Severi, A. Svensson, B. Vinther, E. W. Wolff, The Antarctic ice core chronology (AICC2012): An optimized multi-parameter and multi-site dating approach for the last 120 thousand years. *Clim. Past* **9**, 1733–1748 (2013). doi:10.5194/cp-9-1733-2013

64. P. Köhler, C. Nehrbass-Ahles, J. Schmitt, T. F. Stocker, H. Fischer, A 156 kyr smoothed history of the atmospheric greenhouse gases CO_2, CH_4, and N_2O and their radiative forcing. *Earth Syst. Sci. Data* **9**, 363–387 (2017). doi:10.5194/essd-9-363-2017

65. L. E. Lisiecki, J. V. Stern, Regional and global benthic $\delta^{18}O$ stacks for the last glacial cycle. *Paleoceanography* **31**, 1368–1394 (2016). doi:10.1002/2016PA003002

66. C. Pearce, J. T. Andrews, I. Bouloubassi, C. Hillaire-Marcel, A. E. Jennings, J. Olsen, A. Kuijpers, M. S. Seidenkrantz, Heinrich 0 on the east Canadian margin: Source, distribution, and timing. *Paleoceanography* **30**, 1613–1624 (2015). doi:10.1002/2015PA002884

67. A. Montelli, S. P. S. Gulick, L. L. Worthington, A. Mix, M. Davies-Walczak, S. D. Zellers, J. M. Jaeger, Late Quaternary glacial dynamics and sedimentation variability in the bering trough, gulf of Alaska. *Geology* **45**, 251–254 (2017). doi:10.1130/G38836.1

68. L. Tarasov, W. R. Peltier, A calibrated deglacial drainage chronology for the North American continent: Evidence of an Arctic trigger for the Younger Dryas. *Quat. Sci. Rev.* **25**, 659–688 (2006). doi:10.1016/j.quascirev.2005.12.006

69. L. Tarasov, A. S. Dyke, R. M. Neal, W. R. Peltier, A data-calibrated distribution of deglacial chronologies for the North American ice complex from glaciological modeling. *Earth Planet. Sci. Lett.* **315-316**, 30–40 (2012). doi:10.1016/j.epsl.2011.09.010

70. S. J. Fallon, L. K. Fifield, J. M. Chappell, The next chapter in radiocarbon dating at the Australian National University: Status report on the single stage AMS. *Nucl. Instruments Methods Phys. Res. Sect. B Beam Interact. with Mater*. *Atoms* (2010). 10.1016/j.nimb.2009.10.059

71. T. P. Guilderson, J. R. Southon, T. A. Brown, High-precision AMS ^{14}C results on the TIRI/FIRI turbidite. *Radiocarbon* **45**, 75–80 (2003). doi:10.1017/S0033822200032409

72. M. L. Penkrot, J. M. Jaeger, E. A. Cowan, G. St-Onge, L. LeVay, Multivariate modeling of glacimarine lithostratigraphy combining scanning XRF, multisensory core properties, and CT imagery: IODP Site U1419. *Geosphere* **14**, 1935–1960 (2018). doi:10.1130/GES01635.1

73. J. Haslett, A. Parnell, A simple monotone process with application to radiocarbon-dated depth chronologies. *J. R. Stat. Soc. Ser. C Appl. Stat.* **57**, 399–418 (2008). doi:10.1111/j.1467-9876.2008.00623.x

74. J. Muglia, L. C. Skinner, A. Schmittner, Weak overturning circulation and high Southern Ocean nutrient utilization maximized glacial ocean carbon. *Earth Planet. Sci. Lett.* **496**, 47–56 (2018). doi:10.1016/j.epsl.2018.05.038

75. M. Stuiver, H. A. Polach, Discussion Reporting of ^{14}C data. *Radiocarbon* **19**, 355–

363 (1977). doi:10.1017/S0033822200003672

76. L. A. Krissek, Late Cenozoic ice-rafting records from Leg 145 Sites in the North Pacific: Late Miocene onset, Late Pliocene intensification, and Pliocene-Pleistocene events, in *Proceedings of the Ocean Drilling Program, 145 Scientific Results*, D. K. Rea, I. A. Basov, D. W. Scholl, J. F. Allan, Eds.(Ocean Drilling Program, College Station, TX, 1995), pp. 179–194.

77. H. Cheng, R. Lawrence Edwards, C. C. Shen, V. J. Polyak, Y. Asmerom, J. Woodhead, J. Hellstrom, Y. Wang, X. Kong, C. Spötl, X. Wang, E. Calvin Alexander Jr., Improvements in [230]Th dating, [230]Th and [234]U half-life values, and U-Th isotopic measurements by multi-collector inductively coupled plasma mass spectrometry. *Earth Planet. Sci. Lett.* **371-372**, 82–91 (2013). doi:10.1016/j.epsl.2013.04.006

ACKNOWLEDGMENTS

SUPPLEMENTARY MATERIALS

science.sciencemag.org/cgi/content/full/science.aba7096/DC1
Materials and Methods
Figs. S1 to S15
Tables S1 to S10
References (*67–77*)

26 December 2019; accepted 17 September 2020
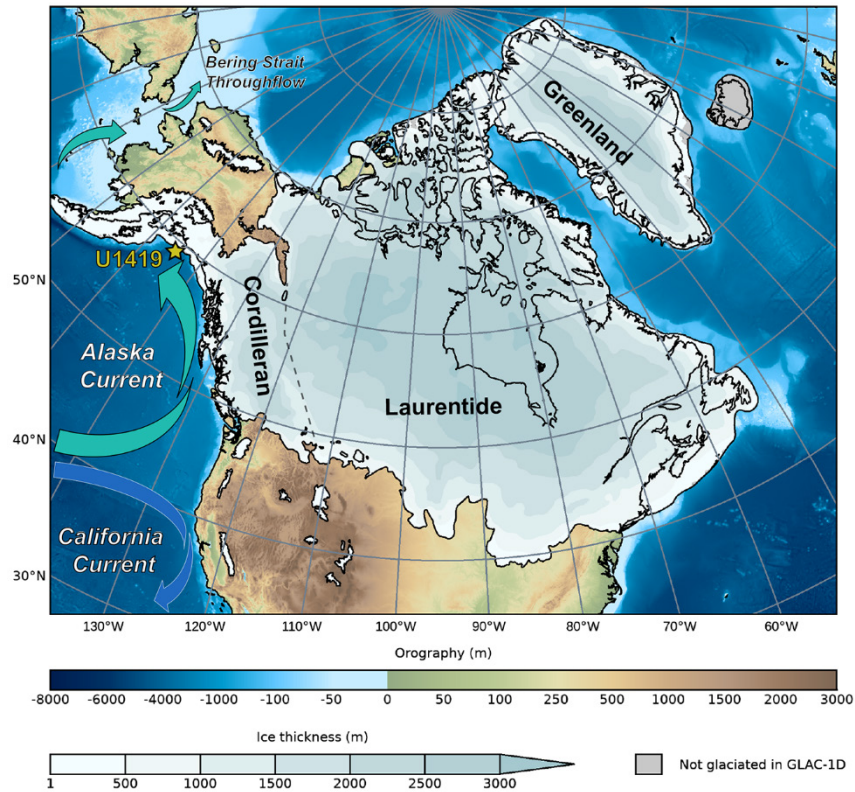Published online 1 October 2020
10.1126/science.aba7096

Fig. 1. Map showing study area. Location of International Ocean Discovery Program Expedition 341 Site U1419 (59° 31.9'N, 144° 8.0'W; 698 m depth) is shown on modern ETOPO1 bathymetry (*58*). The GLAC-1D modeled Last Glacial Maximum (LGM) thickness of the Cordilleran, Laurentide, and Greenland ice sheets is shown (*59*), with margins constrained by the proxy-derived LGM ice extent (*60*). The North American ice sheet saddle separating the Cordilleran from the Laurentide is delineated as a dashed black line. Approximate directions and extent of major NE Pacific surface currents, including the Alaska Current, California Current, and Bering Strait Throughflow are also shown.
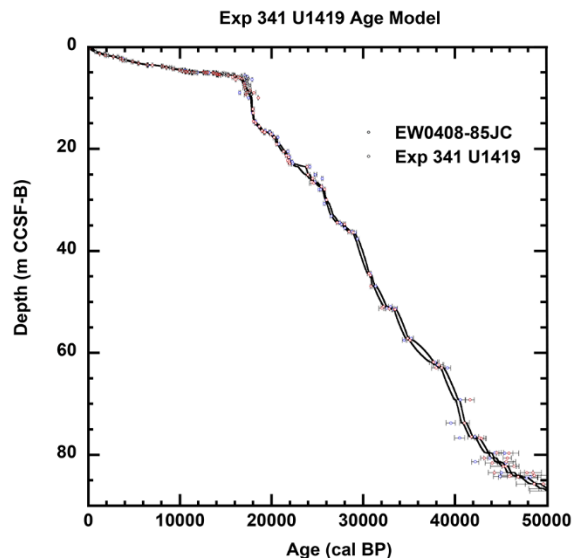
Fig. 2. Bayesian age model for Expedition 341 Site U1419 (see Materials and Methods) based on the Marine13 calibration curve. The solid lines are the ±1-σ error envelope on the age model, shown versus adjusted composite depth below seafloor (CCSF-B) (*17*). All calibrated planktic (blue) and benthic (red) radiocarbon dates are shown. Data from core EW0408-85JC are filled circles (*28*, *33*), while data from U1419 are open circles. See Materials and Methods for Marine20 age model.
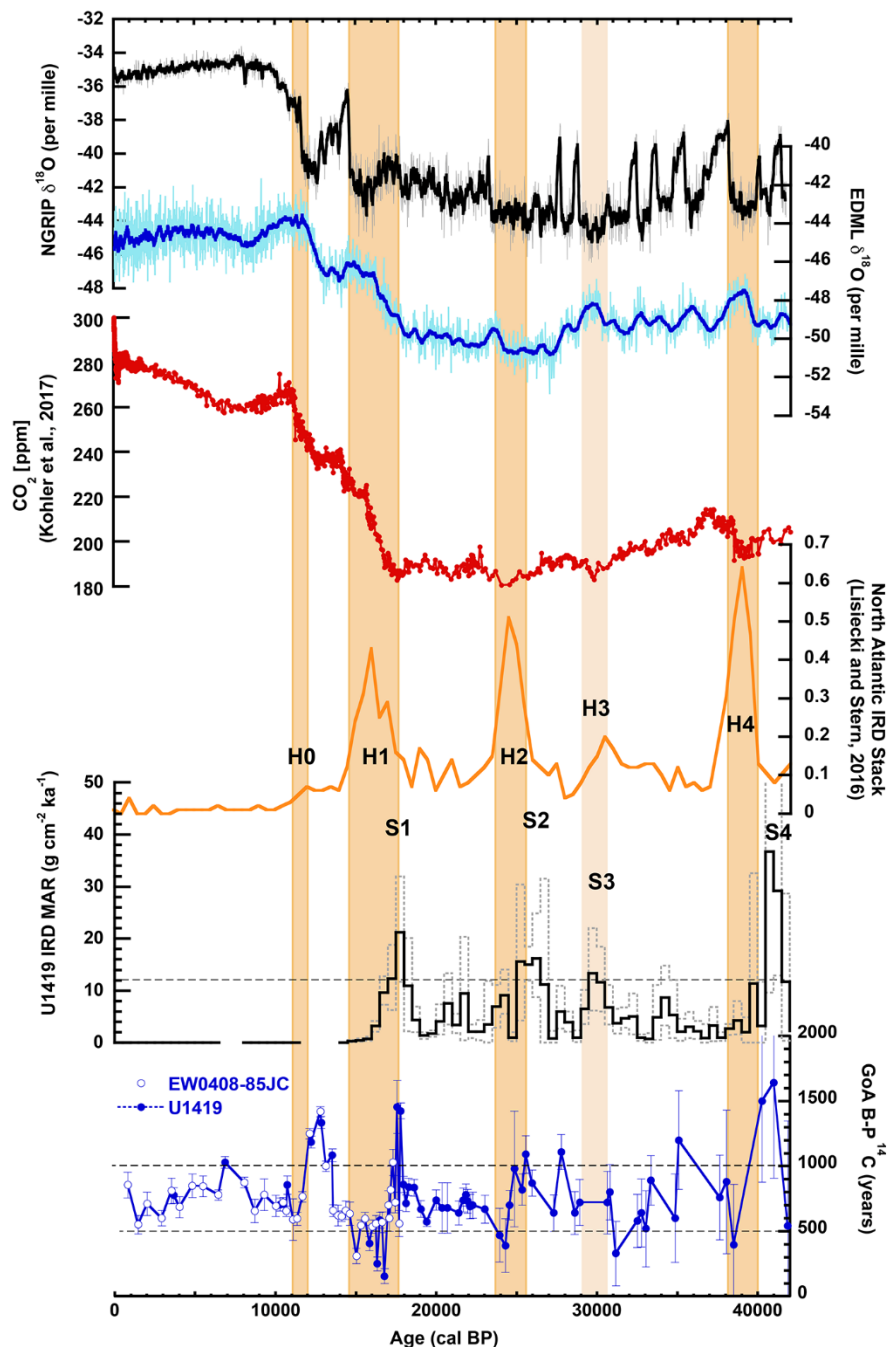
Fig. 3. Global records of climate changes during the latest Pleistocene. Greenland ($\delta^{18}O$ from NGRIP, black; 100 yr smoothing shown in bold) (*61*) and Antarctica ($\delta^{18}O$ from EDML, blue; 100 yr smoothing shown in bold) (*62*) are shown on the synchronized AICC2012 timescale (*63*). Global atmospheric CO_2 from ice cores plotted in red (*64*). Atlantic ice-rafted debris stack (normalized units in orange (*65*)) and U1419 IRD MAR calculated over 500 year increments (black) with $\pm 1\,\sigma$ uncertainty envelope (dashed gray lines). U1419 B-P ^{14}C (Blue, ±1-σ uncertainty; EW0408-85JC data denoted via open symbols). Timing of the North Atlantic Heinrich events shown in light orange bars; H1-H4 from synthesis of (*65*), H0 from (*66*). The dashed line on the U1419 IRD panel denotes the level of 12 g cm^{-2} ka^{-1} that define Siku Events 1-4. The dashed straight lines on the U1419 B-P panel denote 1000 and 500 years; Siku Events are associated with regional B-P ^{14}C age differences in excess of 1000 years, while Heinrich events are associated with values below 500 years.
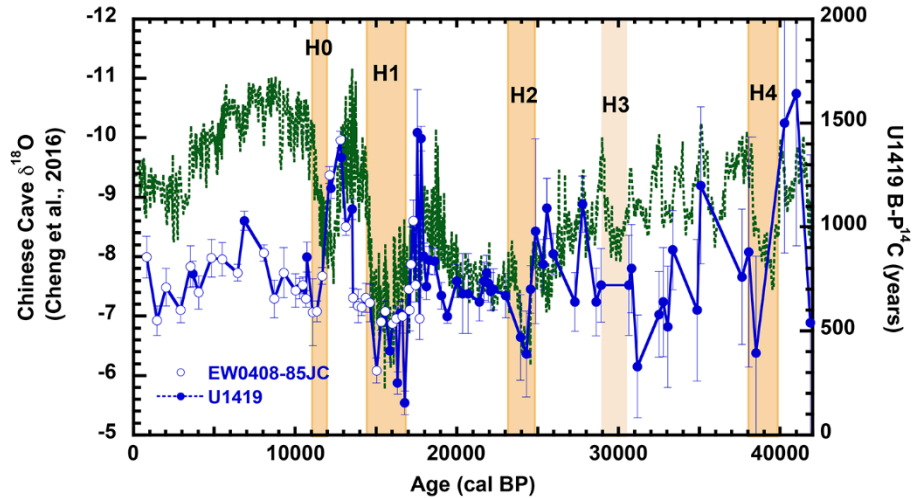
Fig. 4. Paleoclimate connection of the equatorial and high-latitude North Pacific. The B-P ^{14}C record of U1419 (solid blue dots) and its site survey core EW0408-85JC (open blue dots), reflecting changes in the circulation and/or ventilation structure of the intermediate – upper Pacific Ocean, superimposed on the U-Th dated Chinese speleothem δ^{18}O record interpreted as reflecting strength of the Asian monsoon (green dashed line) (*9*). Episodes of high B-P at U1419, and attendant instability of the Cordilleran (Fig. 4) appear to track periods of strong Asian monsoon. Heinrich Events, anomalously low B-P ^{14}C differences, and periods of weak Asian monsoon follow. Timing of the North Atlantic Heinrich events shown in light orange bars; H1-H4 from synthesis of (*65*), H0 from (*66*).
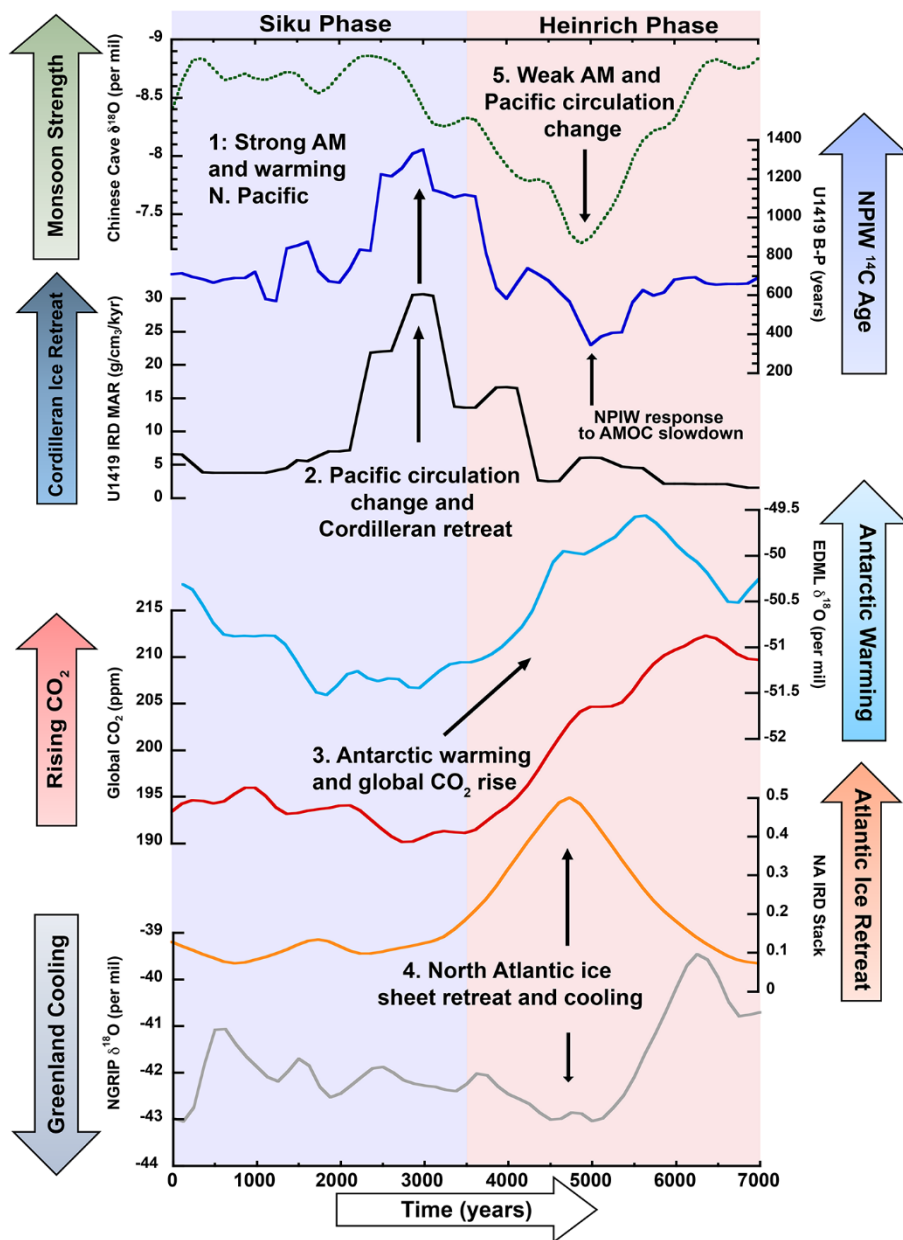
Fig. 5. The progression of global climate anomalies surrounding retreat of the Northern Hemisphere ice sheets over the past ~45,000 cal BP. Canonical events here are averages of the intervals around well-resolved Siku Events 1, 2, and 4 aligned on their published chronologies according to the timing of maxima in ice rafted debris MAR in Site U1419. Each record was then interpolated to 125 yr time step and smoothed with a 750 yr Gaussian filter. The 7000 years of canonical changes surrounding each event are shown for the Asian Monsoon (AM; Chinese Cave speleothem $\delta^{18}O$ (9)), Cordilleran ice-rafted debris (IRD) and Northeast Pacific Intermediate

Science

Phasing of millennial-scale climate variability in the Pacific and Atlantic Oceans

Maureen H. Walczak, Alan C. Mix, Ellen A. Cowan, Stewart Fallon, L. Keith Fifield, Jay R. Alder, Jianghui Du, Brian Haley, Tim Hobern, June Padman, Summer K. Praetorius, Andreas Schmittner, Joseph S. Stoner and Sarah D. Zellers

ARTICLE TOOLS	http://science.sciencemag.org/content/early/2020/09/30/science.aba7096
SUPPLEMENTARY MATERIALS	http://science.sciencemag.org/content/suppl/2020/09/30/science.aba7096.DC1
REFERENCES	This article cites 72 articles, 12 of which you can access for free http://science.sciencemag.org/content/early/2020/09/30/science.aba7096#BIBL
PERMISSIONS	http://www.sciencemag.org/help/reprints-and-permissions

Use of this article is subject to the Terms of Service